CHEMISTRY OF MATERIALS
Article

Chem. Mater. **2010,** *22,* 2239–2247 2239
DOI:10.1021/cm902989f

Surface-Ligand-Dependent Cellular Interaction, Subcellular Localization, and Cytotoxicity of Polymer-Coated Quantum Dots

Shawn J. Tan, Nikhil R. Jana,*,† Shujun Gao, Pranab K. Patra, and Jackie Y. Ying*

Institute of Bioengineering and Nanotechnology, 31 Biopolis Way, The Nanos, Singapore 138669, Singapore. †*Present address: Centre for Advanced Materials, Indian Association for the Cultivation of Science, Kolkata 700032, India.*

Received September 26, 2009. Revised Manuscript Received January 31, 2010

Nanoparticle- and quantum-dot (QD)-based bioprobes are emerging as alternatives to small-molecule probes for in vitro and in vivo applications. However, their cellular interaction and cell uptake mechanism are significantly different from those of small-molecule probes and are extremely sensitive to surface ligands. These present a barrier in the development of nanoparticles and QDs as cellular probes. This work focused on the synthesis of various functionalized QDs with tunable surface charge, hydrophobicity, and functionalization with poly(ethylene glycol) (PEGylation) and their cellular interaction. We found that the surface functional groups of nanometer-sized probes significantly dictated their cellular interaction, subcellular localization, and cytotoxicity. A dose-dependent interaction was observed for all types of QDs, but the cationic surface charge or hydrophobicity would increase the cellular interaction as compared to the anionic surface charge. Cationic QDs rapidly entered cells and induced cytotoxicity, but hydrophobic QDs were stuck to the cell membrane and did not enter the cells. PEGylation of cationic QDs reduced their nonspecific binding and cytotoxicity, and a higher concentration of QDs was required for cellular entry. On the basis of these results, we were able to design different functionalized QD nanoprobes with balanced hydrophobicity and surface charge for cell membrane labeling and subcellular targeting. Mechanistic studies indicated a clathrin-mediated interaction and uptake for all types of QDs. The cellular interaction and uptake of 20−50 nm particles were primarily determined by their surface charges and ability to penetrate the cellular membrane, and the final destinations of the nanoparticles in the cell could be controlled by the appropriate design of surface ligands.

Introduction

Nanoparticle- and quantum-dot (QD)-based probes have gained increasing interest in medical diagnostics and cellular imaging applications.[1−7] The bright, tunable, and photostable optical properties of QDs[4,5] and noble-metal nanoparticles,[1−3] and the interesting magnetic properties of iron oxide nanoparticles[7] offered advantages in optical and magnetic resonance imaging and detection. Functionalized nanoparticles[1−7] could be designed for specific targeting. They might be tailored with single or multiple surface functional groups to increase the labeling specificity or to induce cooperative binding.[8] In cell labeling applications, the controllable fluorescence of QDs has attracted great attention. Recent studies showed that QDs functionalized with bioaffinity probes such as antibodies, peptides, and other small molecules could achieve cell-specific targeting and labeling.[9−38] For example, antibody-functionalized QDs were used to target cell surface receptors[15,16,26] and study protein trafficking.[15,28,35]

*E-mail: jyying@ibn.a-star.edu.sg (J.Y.Y.), camnrj@iacs.res.in (N.R.J.). Fax: (+65) 6478-9020.

(1) Eugenii, K.; Willner, I. *Angew. Chem., Int. Ed.* **2004**, *43*, 6042.
(2) Rosi, N. L.; Mirkin, C. A. *Chem. Rev.* **2005**, *105*, 1547.
(3) Huang, X.; El-Sayed, I. H.; Qian, W.; El-Sayed, M. A. *J. Am. Chem. Soc.* **2006**, *128*, 2115.
(4) Michalet, X.; Pinaud, F. F.; Bentolila, L. A.; Tsay, J. M.; Doose, S.; Li, J. J.; Sundaresan, G.; Wu, A. M.; Gambhir, S. S.; Weiss, S. *Science* **2005**, *307*, 538.
(5) Medintz, I. L.; Uyeda, H. T.; Goldman, E. R.; Mattoussi, H. *Nat. Mater.* **2005**, *4*, 435.
(6) Sun, E. Y.; Josephson, L.; Kelly, K. A.; Weissleder, R. *Bioconjugate Chem.* **2006**, *17*, 109.
(7) Jun, Y.-w.; Huh, Y.-M.; Choi, J.-s.; Lee, J.-H.; Song, H.-T.; Kim, S.; Yoon, S.; Kim, K.-S.; Shin, J.-S.; Suh, J.-S.; Cheon, J. *J. Am. Chem. Soc.* **2005**, *127*, 5732.
(8) Mammen, M.; Choi, S.-K.; Whitesides, G. M. *Angew. Chem., Int. Ed.* **1998**, *37*, 2754.
(9) Bruchez, M.; Moronne, M.; Gin, P.; Weiss, S.; Alivisatos, A. P. *Science* **1998**, *281*, 2013.
(10) Chan, W. C.; Nie, S. *Science* **1998**, *281*, 2016.
(11) Dubertret, B.; Skourides, P.; Norris, D. J.; Noireaux, V.; Brivanlou, A. H.; Libchaber, A. *Science* **2002**, *298*, 1759.
(12) Wu, X.; Liu, H.; Liu, J.; Haley, K. N.; Treadway, J. A.; Larson, J. P.; Ge, N.; Peale, F.; Bruchez, M. P. *Nat. Biotechnol.* **2003**, *21*, 41.
(13) Jaiswal, J. K.; Mattoussi, H.; Mauro, J. M.; Simon, S. M. *Nat. Biotechnol.* **2003**, *21*, 47.
(14) Dahan, M.; Levi, S.; Luccardini, C.; Rostaing, P.; Riveau, B.; Triller, A. *Science* **2003**, *302*, 442.
(15) Lidke, D. S.; Nagy, P.; Heintzmann, R.; Arndt-Jovin, D. J.; Post, J. N.; Grecco, H. E.; Jares-Erijman, E. A.; Jovin, T. M. *Nat. Biotechnol.* **2004**, *22*, 198.
(16) Gao, X.; Cui, Y.; Levenson, R. M.; Chung, L. W. K.; Nie, S. *Nat. Biotechnol.* **2004**, *22*, 969.
(17) Derfus, A. M.; Chan, W. C. W.; Bhatia, S. N. *Adv. Mater.* **2004**, *16*, 961.
(18) Lagerholm, B. C.; Wang, M.; Ernst, L. A.; Ly, D. H.; Liu, H.; Bruchez, M. P.; Waggoner, A. S. *Nano Lett.* **2004**, *4*, 2019.
(19) Chen, F.; Gerion, D. *Nano Lett.* **2004**, *4*, 1827.
(20) Silver, J.; Ou, W. *Nano Lett.* **2005**, *5*, 1445.
(21) Rozenzhak, S. M.; Kadakia, M. P.; Caserta, T. M.; Westbrook, T. R.; Stone, M. O.; Naik, R. R. *Chem. Commun.* **2005**, *17*, 2217.
(22) Delehanty, J. B.; Medintz, I. L.; Pons, T.; Brunel, F. M.; Dawson, P. E.; Mattoussi, H. *Bioconjugate Chem.* **2006**, *17*, 920.
(23) Clarke, S. J.; Hollmann, C. A.; Zhang, Z.; Suffern, D.; Bradforth, S. E.; Dimitrijevic, N. M.; Minarik, W. G.; Nadeau, J. L. *Nat. Mater.* **2006**, *5*, 409.

Published on Web 02/24/2010

Peptide-functionalized QDs were employed to increase the cellular uptake[17−22,27] and subcellular labeling of the nucleus[19] and mitochondria.[17] These studies indicated that targeting cell surface receptors and labeling a specific cell type were more easily attained than subcellular targeting. Microinjection of peptide-functionalized QDs has led to good subcellular specificity, which is typically lost when QDs are taken up through the common endocytotic pathways.[17] Thus, a clear understanding of the cellular uptake mechanism of nanoparticles and QDs and its influence on subcellular localization would be key in the development of cellular and subcellular probes.

Macromolecules, nanoparticles, and microparticles enter into cells via four main endocytotic pathways, i.e., macropinocytosis, clathrin-mediated endocytosis, caveolin-mediated endocytosis, and clathrin- and caveolin-independent endocytosis.[39−41] Although different types of receptors are involved in the different endocytotic mechanisms, clathrin-mediated endocytosis is the most common and well-studied one. There are three general and consecutive steps for cellular internalization: (i) interaction of the particle with the cell membrane, followed by its translocation through the membrane; (ii) incorporation into an endosome; and (iii) sorting via endosomal compartments to subcellular targets such as the Golgi complex, the endoplasmic reticulum or lysosomes.[39−41] The nanoparticle uptake efficiency is determined by the particle-membrane interaction, while the final destination of the nanoparticle is governed by the endocytotic pathway, the nanoparticle's ability for endosomal escape, and the type(s) of ligands on the nanoparticle surface.[42,43]

The first step involves the interaction between the particle and the heparan sulfate proteoglycans and membrane lipids at the cell surface. Because the proteoglycans are negatively charged, the cell surface tends to have stronger electrostatic interactions with cationic particles or polymers. On the other hand, the lipophilic property of membrane lipids allows for stronger interaction with a particle with long-chain hydrocarbons, such as fatty acids and fatty amines. As a result, common cell-penetrating peptides and cell transfection reagents (e.g., lipofectamine) typically possess a positive charge, long-chain hydrocarbons, and/or lipophilicity.[42,43]

Cellular endocytosis, cellular delivery, and subcellular targeting of a nanoparticle-based probe can be influenced in several ways. First, a nanoparticle has a high surface-to-volume ratio, and thus any small change in the particle size, shape and/or surface functional group may lead to significant alteration in cellular interaction.[44−54] Consequently, the cellular uptake, cytotoxicity,[44,45,47,48] and subcellular localization of nanoparticles and QDs are highly sensitive to the particle size,[46,52,53] shape,[52,54] surface charge,[27,44,48,50] hydrophobicity,[36,49] and nature of the surface ligands.[32] Second, a larger probe size (10−100 times that of molecular probes) might lead to a different endocytotic uptake mechanism compared to that of molecular probes.[53] Third, a larger particle size and a higher surface charge would often induce high nonspecific cellular uptake of nanoparticle-based probes,[3,47−50] which further complicated the uptake activity of affinity ligands by reducing the specificity of nanoparticle-based probes. Fourth, nanoparticle-based probes often end up at lysosomes and prevent subcellular targeting.[17] Thus, specially functionalized nanoparticles need to be engineered with endosomal escape and disruption capabilities.[32]

Designing an ideal nanoparticle probe requires a rigorous understanding of the influence of its surface properties on cellular interaction and uptake processes. QD-based probes are ideal for such studies because of their

(24) Zhang, T.; Stilwell, J. L.; Gerion, D.; Ding, L.; Elboudwarej, O.; Cooke, P. A.; Gray, J. W.; Alivisatos, A. P.; Chen, F. F. *Nano Lett*. **2006**, *6*, 800.
(25) Rajan, S. S.; Vu, T. Q. *Nano Lett*. **2006**, *6*, 2049.
(26) Le Gac, S.; Vermes, I.; van den Berg, A. *Nano Lett*. **2006**, *6*, 1863.
(27) Zhang, Y.; So, M. K.; Rao, J. *Nano Lett*. **2006**, *6*, 1988.
(28) Courty, S.; Luccardini, C.; Bellaiche, Y.; Cappello, G.; Dahan, M. *Nano Lett*. **2006**, *6*, 1491.
(29) Gussin, H. A.; Tomlinson, I. D.; Little, D. M.; Warnement, M. R.; Qian, H.; Rosenthal, S. J.; Pepperberg, D. R. *J. Am. Chem. Soc*. **2006**, *128*, 15701.
(30) Zhou, M.; Nakatani, E.; Gronenberg, L. S.; Tokimoto, T.; Wirth, M. J.; Hruby, V. J.; Roberts, A.; Lynch, R. M.; Ghosh, I. *Bioconjugate Chem*. **2007**, *18*, 323.
(31) Yu, W. W.; Chang, E.; Falkner, J. C.; Zhang, J.; Al-Somali, A. M.; Sayes, C. M.; Johns, J.; Drezek, R.; Colvin, V. L. *J. Am. Chem. Soc*. **2007**, *129*, 2871.
(32) Duan, H.; Nie, S. *J. Am. Chem. Soc*. **2007**, *129*, 3333.
(33) (a) Zheng, Y.; Gao, S.; Ying, J. Y. *Adv. Mater*. **2007**, *19*, 376. (b) Zheng, Y.; Yang, Z.; Ying, J. Y. *Adv. Mater*. **2007**, *19*, 1475. (c) Zheng, Y.; Yang, Z.; Li, Y.; Ying, J. Y. *Adv. Mater*. **2008**, *20*, 3410.
(34) Liu, H. Y.; Vu, T. Q. *Nano Lett*. **2007**, *7*, 1044.
(35) Cambi, A.; Lidke, D. S.; Arndt-Jovin, D. J.; Figdor, C. G.; Jovin, T. M. *Nano Lett*. **2007**, *7*, 970.
(36) (a) Selvan, S. T.; Patra, P. K.; Ang, C. Y.; Ying, J. Y. *Angew. Chem., Int. Ed*. **2007**, *46*, 2448. (b) Tan, T. T.; Selvan, S. T.; Zhao, L.; Gao, S.; Ying, J. Y. *Chem. Mater*. **2007**, *19*, 3112.
(37) Chen, I.; Choi, Y.-A.; Ting, A. Y. *J. Am. Chem. Soc*. **2007**, *129*, 6619.
(38) Maysinger, D.; Behrendt, M.; Lalancette-Hebert, M.; Kriz, J. *Nano Lett*. **2007**, *7*, 2513.
(39) Conner, S. D.; Schmid, L. S. *Nature* **2003**, *422*, 37.
(40) Perret, E.; Lakkaraju, A.; Deborde, S.; Schreiner, R.; Rodriguez-Boulan, E. *Curr. Opin. Cell Biol*. **2005**, *17*, 423.
(41) Gruenberg, J.; van der Goot, F. G. *Nat. Rev. Mol. Cell Biol*. **2006**, *7*, 495.
(42) Pujals, S.; Fernández-Carneado, J.; López-Iglesias, C.; Kogan, M. J.; Giralt, E. *Biochim. Biophys. Acta* **2006**, *1758*, 264.
(43) Wasungu, L.; Hoekstra, D. *J. Controlled Release* **2006**, *116*, 255.
(44) Hoshino, A.; Fujioka, K.; Oku, T.; Suga, M.; Sasaki, Y. F.; Ohta, T.; Yasuhara, M.; Suzuki, K.; Yamamoto, K. *Nano Lett*. **2004**, *4*, 2163.
(45) Derfus, A. M.; Chan, W. C. W.; Bhatia, S. N. *Nano Lett*. **2004**, *4*, 11.
(46) Osaki, F.; Kanamori, T.; Sando, S.; Sera, T.; Aoyama, Y. *J. Am. Chem. Soc*. **2004**, *126*, 6520.
(47) Kirchner, C.; Liedl, T.; Kudera, S.; Pellegrino, T.; Javier, A. M.; Gaub, H. E.; Stoelzle, S.; Fertig, N.; Parak, W. J. *Nano Lett*. **2005**, *5*, 331.
(48) (a) Bentzen, E. L.; Tomlinson, I. D.; Mason, J.; Gresch, P.; Warnement, M. R.; Wright, D.; Sanders-Bush, E.; Blakely, R.; Rosenthal, S. J. *Bioconjugate Chem*. **2005**, *16*, 1488. (b) Howarth, M.; Liu, W.; Puthenveetil, S.; Zheng, Y.; Marshall, L. F.; Schmidt, M. M.; Wittrup, K. D.; Bawendi, M. G.; Ting, A. Y. *Nat. Methods* **2008**, *5*, 397. (c) Mok, H.; Bae, K. H.; Ahn, C. H.; Park, T. G. *Langmuir* **2009**, *25*, 1645.
(49) Gopalakrishnan, G.; Danelon, C.; Izewska, P.; Prummer, M.; Bolinger, P.-Y.; Geissbuhler, I.; Demurtas, D.; Dubochet, J.; Vogel, H. *Angew. Chem., Int. Ed*. **2006**, *45*, 5478.
(50) Ryman-Rasmussen, J. P.; Riviere, J. E.; Monteiro-Riviere, N. A. *Nano Lett*. **2007**, *7*, 1344.
(51) Cho, S. J.; Maysinger, D.; Jain, M.; Roeder, B.; Hackbarth, S.; Winnik, F. M. *Langmuir* **2007**, *23*, 1974.
(52) Chithrani, B. D.; Chan, W. C. W. *Nano Lett*. **2007**, *7*, 1542.
(53) Rejman, J.; Oberle, V.; Zuhorn, I. S.; Hoekstra, D. *Biochem. J*. **2004**, *377*, 159.
(54) Geng, Y.; Dalhaimer, P.; Cai, S.; Tsai, R.; Tewari, M.; Minko, T.; Discher, D. E. *Nat. Nanotechnol*. **2007**, *2*, 249.

Scheme 1. Structures of Different Types of Functionalized QDs: (I) Anionic, (II) Hydrophobic Anionic, (III) Cationic, (IV) Hydrophobic Cationic, (V) PEGylated Cationic, and (VI) Hydrophobic PEGylated Cationic

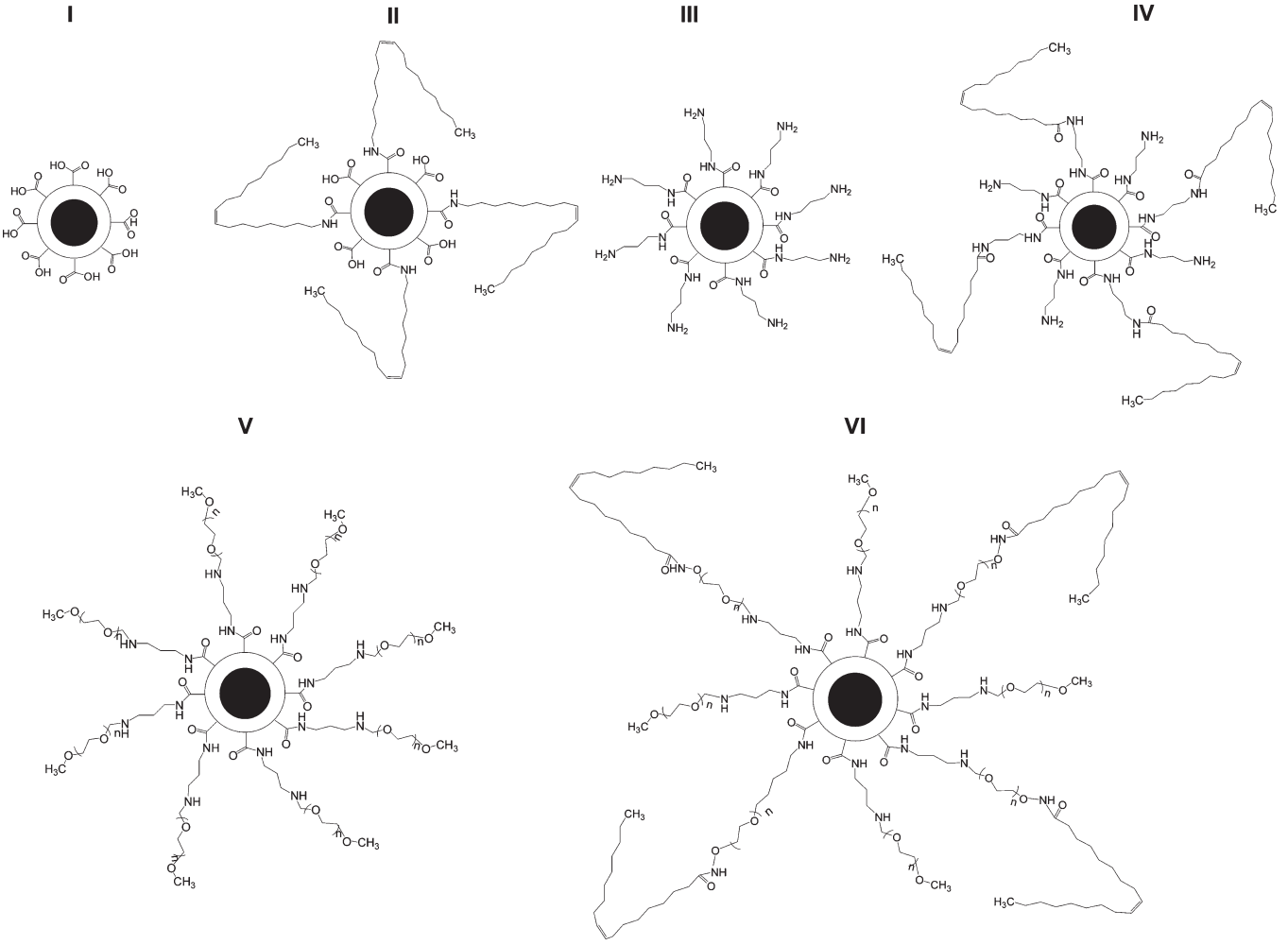

small size and unique fluorescence properties.[4,5] However, the synthesis of QD-based probes with a wide variety of surface chemistry is highly challenging.[4,5] Conventional thiol-based ligand-exchange,[17,33,44,51] polymer coating,[31,32] lipid coating,[11,49] and self-assembly methods[13,22] cannot provide a very broad scope because of the poor colloidal stability of QDs during conjugation chemistry. Alternatively, shell-cross-linked QDs, derived via silica coating[9,19,24,36] or polymer coating,[12,15,16] have been derived with greater promise, but are limited due to a lack of functionalization options as well as issues with nonspecific binding.[47,48,50] We have recently developed polyacrylate/polyacrylamide coating chemistry, which is very powerful in generating a wide range of functionalized nanoparticles with high colloidal stability.[55] The high colloidal stability was attained through the cross-linked shell structure, and a variety of acrylate monomers were employed to introduce different chemical functionalities on the polymer backbone.[55a]

Herein, polyacrylate/polyacrylamide coating chemistry was used to prepare 20−50-nm QDs with different tunable surface charges, hydrophobicity, and functionalization with poly(ethylene glycol) (PEGylation; see Scheme 1). We first tested the cellular interaction and uptake mechanism of these coated QDs in order to understand the role of surface ligands in the interaction and uptake processes. Next, we identified appropriate ligands to develop effective cellular probes for cell membrane labeling and subcellular targeting. We found that interaction with the cell membrane increased for cationic and hydrophobic QDs, as compared to anionic QDs, and in all cases, dose-dependent interaction and clathrin-mediated endocytosis were observed. Confocal microscopy illustrated that hydrophobic particles were localized in cell membranes with very limited intracellular delivery. However, PEGylated hydrophobic particles showed increased intracellular uptake, and PEGylated cationic particles displayed complete intracellular uptake and endosomal localization. This study demonstrated that the initial interaction with the cell membrane was determined by the surface charge and hydrophobicity of nanoparticles but that cellular entry was governed by a balance between hydrophobicity and the surface charge. Our study also illustrated that nonspecific binding, cytotoxicity, cell uptake, and subcellular trafficking were

(55) (a) Jana, N. R.; Ying, J. Y. U.S. Patent Appl. 935644, **2007**, p 60. (b) Jie, Z.; Ting, B. P.; Jana, N. R.; Gao, Z.; Ying, J. Y. *Small* **2009**, *5*, 1414. (c) Wei, Y.; Jana, N. R.; Tan, S. J.; Ying, J. Y. *Bioconjugate Chem.* **2009**, *20*, 1752.

significantly dictated by the surface properties of the nanoprobes, such as the surface charge, surface functional group, and nature of the surface ligands.

Experimental Section

Synthesis of QD Probes. The details of polyacrylate and polyacrylamide coatings were reported earlier.[55a] First, CdSe QDs were prepared by high-temperature pyrolysis of the carboxylate precursors of Cd in an octadecene solvent.[56−58] Next, they were capped by ZnS at 200 °C in octadecene via the alternate injection of zinc stearate in octadecene and elemental S dissolved in octadecene. Next, they were converted into water-soluble, polymer-coated particles via the in situ polymerization of acrylate/acrylamide monomers as follows. Hydrophobic QDs were purified of free surfactants and then dissolved in reverse micelles. Next, the solution was transferred to a three-necked flask, mixed with the monomers, and purged with nitrogen before persulfate was added to initiate the polymerization. Two types of polymer-forming acryl monomers were used for polymer coating, i.e., acrylic acid and *N*-(3-aminopropyl)methacrylamide hydrochloride. The acrylic acid monomer produced polymer-coated particles with surface carboxylic acid groups (I in Scheme 1). The *N*-(3-)methacrylamide monomer led to polymer-coated QDs with primary amine surface groups (III in Scheme 1). The molecular weight of the polymer coating was found by MALDI mass spectroscopy to range from 40 000 to 70 000.[55] Thermal gravimetric analysis indicated that the polymer coating represented ∼70 wt % of the coated QDs, which could be accounted by approximately seven polymer units on each particle surface.[55] The primary amine functional groups in the amine-functionalized particles have been quantified via fluorescamine titration to vary from several hundreds to several thousands, depending on the amount of amine monomer employed in the synthesis. These results were similar to those reported earlier for the silica-coated nanoparticles.[58b]

Polymer-coated particles I and III were further functionalized to prepare other types of QDs. Hydrophobic QDs (II and IV) were prepared from I and III, respectively, using 1-ethyl-3-[3-(dimethylamino)propyl]carbodiimide hydrochloride (EDC) coupling chemistry. To prepare II, 2.0 mL of an aqueous solution of I (absorbance of ∼0.5 at the first absorption maximum) was mixed with 0.02 mL of an ethanolic solution of oleylamine (0.1 M), and the pH was adjusted to 5.5 using an *N*-(2-hydroxyethyl)piperazine-*N*′-2-ethanesulfonic acid (HEPES) buffer solution. To prepare IV, 2.0 mL of solution III was mixed with 0.02 mL of an ethanolic solution of oleic acid (0.1 M), and the pH was adjusted with a HEPES buffer solution. Next, aqueous EDC (0.1 M) and *N*-hydroxysuccinimide (0.1 M) were freshly prepared separately; 0.2 mL of each solution was added to solutions I and III and incubated overnight. The resulting solutions were then dialyzed overnight to remove excess reagents.

V was prepared by reacting III with methoxypoly(ethylene glycol) butylaldehyde (aldehyde-PEG; MW 3400, SunBio). Typically, solution III (absorbance of ∼0.5 at the first absorption maximum) was prepared in a borate buffer of pH 9.5 and mixed with aldehyde-PEG (10 mg dissolved in 0.2 mL of water). After 1 h, a freshly prepared aqueous borohydride solution (0.1 M) was added to reduce the unstable imine bond. After 30 min, this solution was dialyzed overnight to remove any unreacted reagents.

VI was prepared by reacting III with aldehyde-PEG oleylamide. The aldehyde-PEG oleylamide was prepared by mixing poly(ethylene glycol) dibutylaldehyde (MW 3500, SunBio) with an equivalent amount of oleylamine. Typically, 1 mL of a borate buffer (pH 9.5) solution of poly(ethylene glycol) dibutylaldehyde (0.01 M) was mixed with 0.1 mL of an ethanolic solution of oleylamine (0.1 M). After 30 min, 0.5 mL of this solution was mixed with a sample III solution (absorbance of ∼0.5 at the first absorption maximum) in a borate buffer of pH 9.5. Next, the borohydride reduction of imine and dialysis were performed. A similar reaction was conducted to control the number of oleyl groups on the QD surface. A mixture of aldehyde-PEG and aldehyde-PEG oleylamide with a different molar ratio was reacted with III, followed by borohydride reduction and dialysis.

For NMR sample preparation, the dialyzed QD samples were vacuum-dried and dissolved in D_2O.

Cell Labeling Study. HepG2 and NIH3T3 cells grown in a cell culture flask [using Dulbecco's modified Eagle's medium (DMEM) as the medium] were subcultured in 24-well plates (with 0.5 mL of the culture medium for each plate). For confocal microscopy studies, cells were cultured on a circular coverslip placed under the cell culture plate. The cells were attached to the culture plate or coverslip overnight. They were next incubated with 10−100 μL of a QD solution (∼0.1 mg/mL) for 1−2 h. The cells were then washed with phosphate-buffered saline (PBS) twice and used for imaging. For imaging experiments, the same excitation wavelength and exposure time were employed for comparative study. The entire quantitative study of uptake was performed by flow cytometry (FACS).

Colocalization Study. Each experiment was conducted for the following four sets: (i) QD sample; (ii) lysotracker red; (iii) a QD and lysotracker red mixture; and (iv) no QD and no lysotracker red. The cells were first washed with PBS (1×) and replaced with serum-free media. Next, QDs, lysotracker red (∼5 nM), or the QD−lysotracker red mixture was introduced and incubated with the cells for 1 h, 15 min, or 1 h, respectively. The cells were then washed two or three times with PBS (1×) and used for imaging.

Dose-Dependent Study. Most studies were performed with final QD concentrations of 5, 25, and 50 nM. The QD concentration was determined based on the absorbance value at the first absorption maximum, using the molar extinction coefficient determined earlier.[59] Cells were washed with PBS (1×) and replaced with serum-free media. Next, QDs of different amounts were introduced and incubated for 1 h. The cells were then washed with PBS (1×) and trypsinized to detach from the well plate. They were transferred into 15 mL centrifuge tubes containing ∼2 mL of complete media for trypsin inactivation. Next, the cells were separated by centrifugation at 1000 rpm for 5 min. The precipitated cells were collected after removal of the supernatant, resuspended in 2 mL of PBS (1×) for washing, and centrifuged again at 1000 rpm for 5 min. The resulting cell precipitate was collected, resuspended in 1 mL of PBS (1×), and used for flow cytometry analysis. Approximately 10 000−20 000 cells were used for each sample analysis, and the raw flow cytometry data were obtained as a frequency histogram of the relative fluorescence plotted against the number of events. The quantitative cellular interaction and uptake were determined from the raw flow cytometry data after subtraction of the

(56) Li, J. J.; Wang, Y. A.; Guo, W.; Keay, J. C.; Mishima, T. D.; Johnson, M. B.; Peng, X. *J. Am. Chem. Soc.* **2003**, *125*, 12567.
(57) Selvan, S. T.; Tan, T. T.; Ying, J. Y. *Adv. Mater.* **2005**, *17*, 1620.
(58) (a) Jana, N. R.; Earhart, C.; Ying, J. Y. *Chem. Mater.* **2007**, *19*, 5074. (b) Jana, N. R.; Yu, H.-h.; Mohamed Ali, E.; Zheng, Y.; Ying, J. Y. *Chem. Commun.* **2007**, 1406.
(59) Yu, W. W.; Qu, L.; Guo, W.; Peng, X. *Chem. Mater.* **2003**, *15*, 2854.

contribution from the control cells without QDs. The control sample showed some signal due to cellular autofluorescence [see Figure S1 in the Supporting Information (SI)].

Endocytotic Inhibition Study. Each study included a negative control (i.e., no QDs and no inhibitors), a positive control (with QDs only and no inhibitors), and the QD sample with a specific inhibitor. The experiments generally required two or three confluent wells (in a 24-well plate) for each sample tested. The inhibitors used are summarized below. For the inhibition study, cells were washed with PBS (1×) buffer and replaced with serum-free media. Next, the inhibitor solution was added and incubated for 30 min. The QD solution was then added and incubated for 15−60 min. The cells were then washed and used for FACS analysis, as described for the dose-dependent study.

inhibitor	concentration (μg/mL)	process inhibited
CHP	15	clathrin-mediated endocytosis
MBCD	15	non-clathrin-mediated endocytosis
nystatin	30	clathrin-mediated endocytosis
amiloride	1.5	macropinocytosis
genistein	50	caveolae-mediated endocytosis
cytochalasin D	2.5	macropinocytosis, caveolae uptake

Cell Viability Study by 1-Methyltetrazole-5-thiol (MTT) Assay. HepG2 and NIH3T3 cells were trypsinized and resuspended in DMEM with 10% fetal bovine serum and 1% penicillin/streptomycin. The cells were seeded on a 96-well flat-bottomed microplate in 100−200 μL of a full DMEM culture medium and kept overnight at 37 °C and 5% CO_2. QDs of different concentrations were loaded into each well, with six duplicates for each QD concentration. Each system was incubated for 24, 48, and 72 h; 20 μL of a MTT solution (5 mg/mL) was added to each well 4 h before the end of the incubation period. The medium was discarded by aspiration, and formazan was dissolved with 200 μL of dimethyl sulfoxide. The plates were read for absorbance at 550 nm. The optical density was directly correlated with the cell quantity, and the cell viability was calculated by setting the cell viability of the control set (without any QDs) as 100%. To examine the toxic effects of different ligands, 5 nm iron oxide nanoparticles with similar polymer coating were also prepared for the cytotoxicity study. The hydrophobic iron oxide nanoparticles were synthesized using our published protocol[60] and then coated with polyacrylate like that for the QDs.[55a]

Instrumentation. Ultraviolet−visible absorption spectra were recorded using an Agilent 8453 spectrophotometer in a 1 cm quartz cell. Fluorescence spectra were obtained with a Jobin Yvon Horiba Fluorolog fluorescence spectrometer. The quantum yield (QY) was measured using the integrated fluorescence intensity of the QD and reference (fluorescein, QY = 97%) under 470 nm excitation. A concentrated solution (5−10 mg/mL) was used to acquire NMR spectra (Bruker AV-400 instrument, 400 MHz). Solid samples were characterized by photoacoustic Fourier transform infrared (FTIR) spectroscopy. For dynamic light scattering (DLS) studies, samples were first filtered through a PALL syringe filter (0.1 μm pores) and then characterized with a Brookhaven Instrument Corp. model BI-200SM instrument. Cell imaging was performed using an Olympus microscope IX71 with a DP70 digital camera. Confocal fluorescence imaging was conducted using an Olympus Fluoview 300 confocal laser scanning system with 488 nm laser excitation. A BD FACS Calibur flow cytometer (with four-color basic modular flow) was employed for quantification of the cellular uptake.

(60) Jana, N. R.; Chen, Y.; Peng, X. *Chem. Mater.* **2004**, *16*, 3931.

Results and Discussion

The chemical structures of our functionalized QDs are shown in Scheme 1. Carboxylate QDs (I) and amine-functionalized QDs (III) were synthesized with our polymer coating scheme, using acrylic acid and *N*-(3-aminopropyl)methacrylamide as polymer-forming precursors, respectively. QDs I and III were further functionalized to derive other functionalized QDs. Oleyl-functionalized hydrophobic anionic QDs (II) were synthesized by reacting I with oleylamine, using EDC coupling chemistry. Similarly, oleyl-functionalized hydrophobic cationic QDs (IV) were prepared by reacting III with oleic acid, using EDC coupling chemistry. PEGylated cationic QDs (V) were derived by reacting III with aldehyde-PEG. Hydrophobic PEGylated cationic QDs (VI) were synthesized by reacting III with aldehyde-PEG oleylamide. The chemical structures of the functionalized QDs were confirmed with NMR spectroscopy and FTIR spectroscopy (see Figure S2 and Table S1 in the SI). NMR and FTIR spectroscopies were also employed to verify that the original ligands used in the QD synthesis (e.g., trioctylphosphine, trioctylphosphine oxide, octadecylamine, and stearic acid) were completely removed from the functionalized QDs (see the SI). The surface charge of QDs was characterized with ζ-potential measurements, and the overall nanoparticle size in solution was determined by DLS (Table 1). I and II were negatively charged, but the other QD samples were positively charged at pH 7.0 in PBS (1×). The surface charge of the QDs could be altered depending on the solution pH and ionic strength, although the influence of the pH was more dominant than that of the ionic strength. We have employed PBS (1×) buffer of pH 7.0 in most of our studies. All QD solutions were optically transparent and colloidally stable in PBS buffer for ≥6 months. The colloidal stability of II and IV was sensitive to the amount of oleyl groups on their surfaces. Because excessive oleyl groups would lead to water-insoluble QDs, partial oleyl functionalization was adopted. The QYs of the QDs were determined to be 15−40%, depending on the QD core size and coating.

To examine the QDs' cellular interaction, HepG2 and NIH3T3 were used as model cell lines. Both cell lines behaved similarly to our QDs; thus, we will discuss mainly the results obtained with the HepG2 cells. Figure 1 shows the representative fluorescence labeling of HepG2 with different QDs. The live cells were incubated with QDs at 37 °C in cell culture media for ∼1 h. The free QDs were then washed away, and fresh media were added before imaging. Imaging studies illustrated that the cellular interactions of QDs were sensitive to their surface charge, hydrophobicity, and PEGylation. Except for I, all of the QDs were attached to the cells, but III and IV were very toxic to the cells (see Table 1). These findings indicated that the anionic QDs have weaker interactions with cells

Table 1. Characteristics of Different Types of Functionalized QDs

QD	DLS size (nm)	ζ potential (mV)	cellular uptake	subcellular localization	cytotoxicity (tolerance dosage)[a]
I, anionic	20 ± 5	-29	low		low (100 nM)
II, hydrophobic anionic (derived from I)	20 ± 10	-25	medium	cell membrane	medium (10 nM)
III, cationic	30 ± 10	$+33$	high	cell membrane, lysozome	high (2 nM)
IV, hydrophobic cationic (derived from III)	35 ± 10	$+26$	high	cell membrane	high (2 nM)
V, PEGylated cationic (derived from III)	20 ± 5	$+8$	medium	lysozome	low (50 nM)
VI, hydrophobic PEGylated cationic (derived from III)	30 ± 10	$+10$	high	cell membrane, lysozome	medium (10 nM)

[a] The tolerance dosage corresponded to >90% viability of the HepG2 cells after 12 h of incubation.

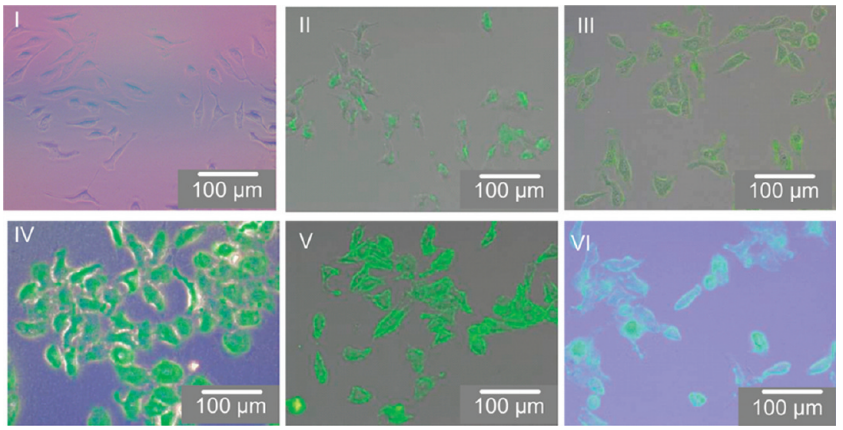

Figure 1. Representative fluorescence micrographs of different types of functionalized QDs: (I) anionic, (II) hydrophobic anionic, (III) cationic, (IV) hydrophobic cationic, (V) PEGylated cationic, and (VI) hydrophobic PEGylated cationic.

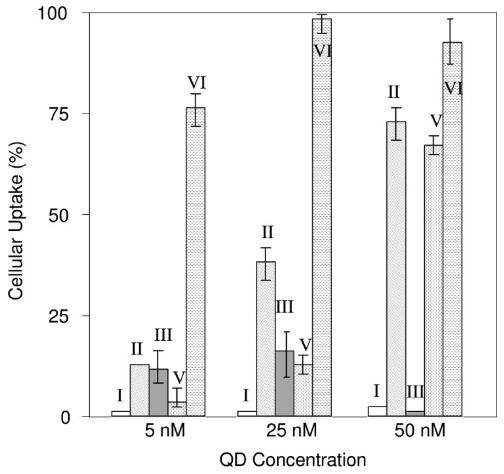

Figure 2. Dose-dependent interaction and uptake of different types of functionalized QDs (from left to right): (I) anionic, (II) hydrophobic anionic, (III) cationic, (V) PEGylated cationic, and (VI) hydrophobic PEGylated cationic. Note that "100%" represents that all cells are labeled.

than the hydrophobic and cationic QDs. Flow cytometry was used to quantify the dose-dependent interactions between the QDs and cells. Cells were incubated with different concentrations of QDs, washed, and analyzed by flow cytometry. The quantitative cellular interaction and uptake were determined after subtraction of the signal contribution from cellular autofluorescence. Figure 2 shows a dose-dependent cellular interaction of QDs at nanomolar concentrations. Because of severe cytotoxicity, we did not perform the flow cytometry study on IV and noted that the dose-dependent studies were conducted above the tolerance dosage of III (see Table 1). We note also that cellular interactions increased drastically with the introduction of hydrophobic oleyl groups on the QD surface. For example, a comparison of I and II illustrated that the cellular interaction of anionic QDs could be increased by 5−20 times after oleyl functionalization. Another significant observation was that PEGylation led to decreased nonspecific binding and reduced the cellular interactions of QDs, as observed earlier.[48] PEGylation (V) of cationic QDs (III) lowered their cellular interaction and thus decreased their cytotoxicity. For example, the comparison of III and V in Figure 2 showed that PEGylation reduced the cellular labeling to $^1/_3$ at 5 nM but allowed for efficient labeling at 50 nM, whereas non-PEGylated QD was highly toxic. The most interesting finding was associated with the hydrophobic PEGylated cationic QDs (VI). The oleyl groups increased the cellular interactions, while the PEG coating reduced the cytotoxicity. Thus, VI was a very effective label even when it was employed at a low concentration of 5 nM.

Because I was used to derive II and III was used to derive IV−VI, we could compare the cellular interaction characteristics of I with II and III with IV−VI (see Table 1). In contrast, a comparison between I and II with III−VI would not be straightforward because I and II were anionic, while III−VI were cationic.

Cytotoxicity studies were performed by MTT assay (Figure 3). The cell viability of QDs was found to be very sensitive to the surface coating. Cationic QDs with primary amine groups (III) were very toxic even at 12.5 nM,

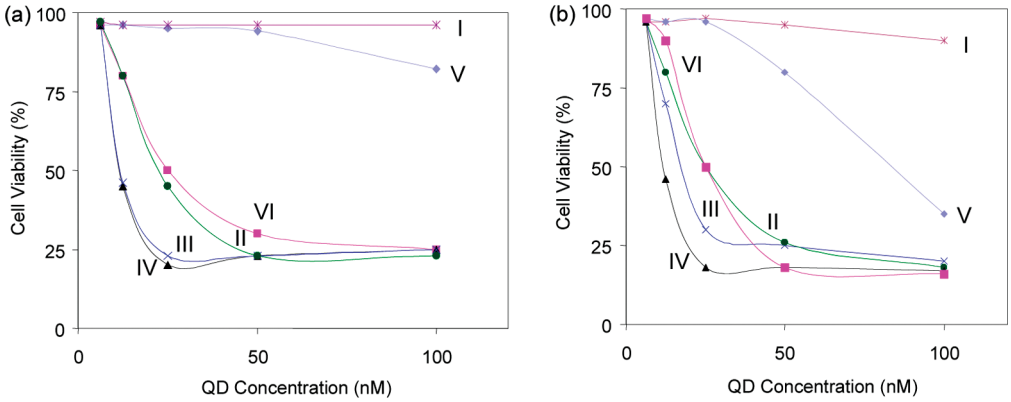

Figure 3. Cytotoxicity on (a) NIH3T3 and (b) HepG2 after 24 h with different types of functionalized QDs: (I) anionic, (II) hydrophobic anionic, (III) cationic, (IV) hydrophobic cationic, (V) PEGylated cationic, and (VI) hydrophobic PEGylated cationic.

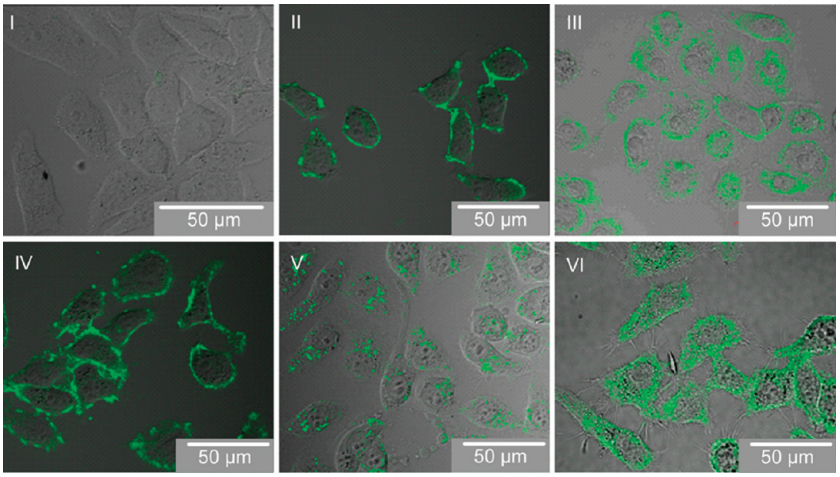

Figure 4. Confocal micrographs showing the subcellular localization after 1 h with different types of functionalized QDs: (I) anionic, (II) hydrophobic anionic, (III) cationic, (IV) hydrophobic cationic, (V) PEGylated cationic, and (VI) hydrophobic PEGylated cationic. The cationic QDs (III) were incubated with the cells for a short time (~10 min instead of 1 h) to ensure membrane labeling and low cytotoxicity.

while anionic QDs with carboxylate groups (I) have almost no toxic effect at ≤100 nM. PEGylation of cationic QDs improved the cell viability significantly, while oleyl groups led to highly toxic QDs. Hydrophobic PEGylated cationic QDs (VI) have intermediate cytotoxicity. The tolerance dosages of different QDs were determined from >90% viability of HepG2 cells after 12 h of incubation (see Table 1). It was apparent that the cytotoxicity of QDs was related to their cellular interactions and uptake. For example, the reduced cytotoxicity of anionic QDs (I) and PEGylated QDs (V) was due to their poor interactions with cells. The higher cytotoxicity of hydrophobic QDs (II, IV, and VI) and cationic QDs (III) could be attributed to their stronger cellular interactions and internalization by the cells. We have also tested the cytotoxicity of iron oxide nanoparticles coated with different types of functional ligands in order to determine whether the toxic effect was due to the QDs or the ligands (Figure S3 in the SI). This control experiment showed that the cytotoxicity of the differently functionalized iron oxide nanoparticles was similar in trend and quite similar in magnitude to that of the differently functionalized QDs. Because iron oxide nanoparticles were well-known to be nontoxic, these control studies suggested that the cytotoxicity could be mainly attributed to the surface ligands rather than the QDs themselves. The low toxicity of our QDs was expected given the low concentration of QDs employed, and the fact that CdSe was well-capped by ZnS to minimize any toxic Cd release. However, other toxic effects such as the reactivity of QDs would need to be examined in further studies.[61]

Confocal microscopy was employed to examine the subcellular localization of QDs. Figure 4 shows that cell labeling was not achieved with I because of its poor interaction with cells. The other functionalized QDs were able to label the cells, although localization of the QDs was different for the different types of functionalized QDs. Oleylated QD labeled mainly the cell membrane, without significant cell internalization. Control experiments were also conducted, and it was found that membrane-labeled QDs (II) did not enter cytoplasm even after 24 h. In contrast, cationic QD (III) labeled the cell membrane first and then entered the cells within 15 min. This study concluded that oleylated QDs were bound

(61) (a) Schneider, R.; Wolpert, C.; Guilloteau, H.; Balan, L.; Lambert, J.; Merlin, C. *Nanotechnology* **2009**, *20*, 225101. (b) Dumas, E.-M.; Ozenne, V.; Mielke, R. E.; Nadeau, J. L. *IEEE Trans. Nanobiosci.* **2009**, *8*, 58.

strongly to the cell membrane. A completely different type of localization was observed for PEGylated cationic QDs (V). They entered the cells within 1 h and did not label the cell membrane. Introduction of oleyl groups on the PEGylated QDs (VI) led to the localization of QDs both in the cell membrane and within the cells. Colocalization studies with lysotracker red indicated that a significant fraction of the QDs was localized in the lysozome (see Figure S4 in the SI). Cationic QDs (III) first localized at the cell membrane and then entered the cytoplasm within 15 min; further studies were difficult because of the high cytotoxicity of III.

To understand the endocytosis mechanism, we have studied the quantitative cellular interaction and uptake of QDs in the presence of different inhibitors, such as chloropromazine (CHP), methyl-β-cyclodextrin (MBCD), nystatin, amiloride, genistein, and cytochalasin D. It is well-known that CHP and nystatin inhibit clathrin-mediated endocytosis, amiloride inhibits macropinocytosis, genistein inhibits caveolae-mediated endocytosis, MBCD inhibits non-clathrin-mediated endocytosis, and cytochalasin D inhibits macropinocytosis and caveolae uptake.[40] Cells were incubated with QDs and inhibitors simultaneously in the cell culture medium for ~1−2 h. Next, the cells were washed with a buffer solution and analyzed by flow cytometry. Hydrophobic anionic QDs (II), PEGylated cationic QDs (V), and hydrophobic PEGylated cationic QDs (VI) were examined. The other QD systems were not tested because of their cytotoxicity (III and IV) or poor cellular interactions (I). Figure 5 shows that, among all inhibitors, CHP has the most significant effect, reducing the cellular uptake significantly. The other inhibitors did not alter the cellular uptake process substantially. Because CHP inhibited the clathrin-mediated endocytosis processes,[39−41] we deduced that the interaction and uptake processes of hydrophobic anionic, PEGylated cationic, and hydrophobic PEGylated cationic QDs were clathrin-mediated.

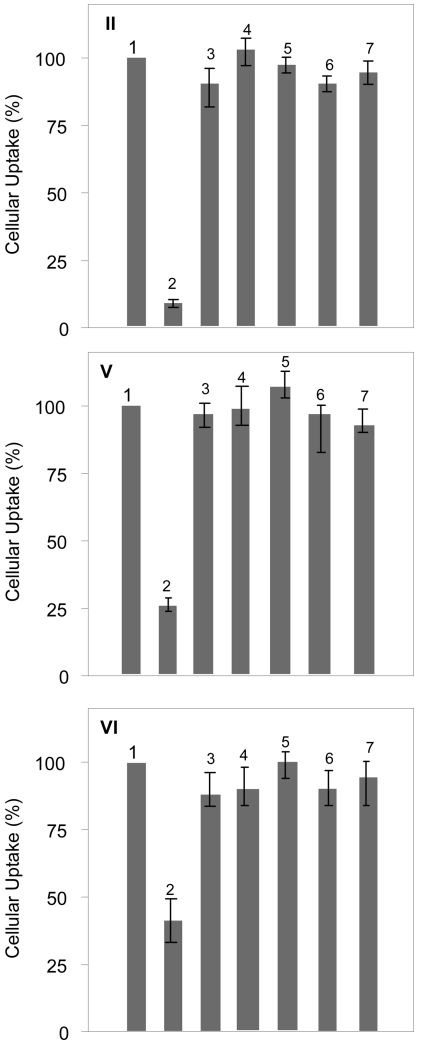

Figure 5. Cellular interaction and uptake of (II) hydrophobic anionic QDs, (V) PEGylated cationic QDs, and (VI) hydrophobic PEGylated cationic QDs in the presence of (1) no inhibitor, (2) CHP, (3) MBCD, (4) nystatin, (5) amiloride, (6) genistein, and (7) cytochalasin D.

Our studies provided insight into the origin of nanoparticles' interactions with cells and the factors involved. While small molecules and ions can traverse the plasma membrane via protein pumps or channels, internalization of macromolecules and particles occurs through endocytosis. The complexity of endocytosis reflects the great evolutionary effort toward control of the entry of foreign materials into the cells in response to the environment. Consequently, phagocytosis (uptake of larger particles) occurs on specialized cells (e.g., macrophages), while pinocytosis (uptake of smaller particles and macromolecules) takes place either on specialized cells (e.g., caveolae-mediated endocytosis in endothelial cells) or through the receptor-mediated uptake process. Among the different types of pinocytosis, clathrin-mediated endocytosis is the most common in mammalian cells and is responsible for the continuous uptake of essential nutrients, intercellular communications, and signal transduction. Thus, it was not surprising that the interaction and uptake of 20−35 nm QDs was associated with clathrin-mediated endocytosis processes. Lysosomal localization of QDs indicates that the QDs are rooted in the endocytic vesicles during the clathrin-mediated endocytosis, are unable to escape from there, and are finally trapped in lysosomes.[39−41] Similar types of endocytosis have also been observed by others for both QDs and nanoparticles.[4,5,17,32,53] This study showed that cationic, anionic, and hydrophobic nanoparticles of 20−35 nm were uptaken through clathrin-mediated pathways and then trapped in the lysosomes.

Our experimental findings offered a general insight into nanoparticles' interaction with cells. The immediate barrier for particle entry is the cell membrane, which is a dynamic self-assembled structure consisting of lipids. Earlier work on the pathogen entry and drug/gene delivery shows that the hydrophobicity and cationic nature of a protein, peptide, or polymer can induce greater interaction with cell membrane, such as that observed in the transfection agent for the effective cellular delivery of drugs, DNA, and proteins.[42,43] For example, cell-penetrating peptides have basic amino acids (such as arginine and histidine), along with hydrophobic peptide sequences. Similarly, conventional cell

transfection agents have secondary and tertiary amine functional groups, along with long-chain hydrophobic segments.[42,43] Thus, it was not unexpected that the cationic oleyl-functionalized QDs have greater cellular interactions and uptake. However, the type of cellular interaction with our QD probes was significantly different from that with the molecular probes. First, the hydrophobic QDs were stuck permanently on the cell membrane, whereas oleylated molecular probes were able to enter the cells. Second, it was possible to tune the interaction and cellular entry of QDs via the surface ligands. For example, with increases in the percentage of oleyl groups on the PEGylated QD surface, cellular interaction could be modulated between complete cell internalization and complete cell membrane labeling.

Oleyl-functionalized molecular probes and nanoparticles have been widely employed because of their strong interactions with lipidic cell membranes.[36a,42,43] The role of the cationic nature of peptides, transfection agents, and polymers has also been well-studied. The strong interaction of cationic amino groups with negatively charged cell surface glycoprotein is considered to be the origin of the high cellular interaction and uptake.[42] However, the cellular interaction of oleylated cationic molecular probes and of oleylated cationic QDs was different. Because multiple oleylated cationic groups were present on the QD surface, their interactions with the cell membrane were polyvalent. This led to a much stronger interaction of oleylated cationic QDs with cells, permanent immobilization of oleylated QDs on the cell membrane, and high QD cytotoxic effects. In contrast, molecular probes usually consisted of one or two oleyl group(s) and/or a few basic amino groups to provide optimum hydrophobicity and cationic charge that drive interaction with the cell membrane, followed by cell internalization processes without significant cytotoxicity. The advantage of QD-based probes was that the cellular interaction, cytotoxicity, and cellular delivery could be systematically varied via changes of the surface ligands (e.g., as in oleylated PEGylated QDs) and/or by variation of the percentage of surface ligands (e.g., percentage of oleyl groups on PEGylated QDs). The benefit of such tunability has yet to be fully explored.

Another significance of this work was the understanding of nonspecific binding interaction between QDs and cells and how to minimize it.[3,47−50] The cellular interaction of oleylated and cationic QDs was nonspecific due to the lipidic cell membrane and generally anionic cell surface. In fact, we observed a similar nature of interaction with other cell lines, such as NIH3T3 and 4T1. We also found that any electrostatically bound molecule that could induce hydrophobicity or cationic charge could also influence the cellular interaction processes drastically (see Figure S5 in the SI). We performed control experiments for such a purpose and synthesized hydrophobic or cationic QDs via electrostatic interaction. The hydrophobic anionic QDs were prepared by the mixing of anionic QDs (I) with oleylamine, whereby the protonated amine group helped attach oleylamine to the anionic QDs via electrostatic interaction. Similarly, cationic QDs were prepared by the mixing of anionic QDs (I) with poly(ethyleneimine) (MW = 2000). These oleylated and cationic QDs displayed a similarly high interaction with cells, suggesting that simple electrostatic interaction could influence the cellular interaction. Thus, it was important to note that QDs and nanoparticles ought to be extremely pure from electrostatically bound molecules and ions, which would otherwise induce nonspecific interactions in cell labeling. The commonly employed synthesis of QDs and nanoparticles involves surfactants, and any cell labeling materials developed thereof would have to be washed free of such surfactants. Ideal nanoparticle probes should have low surface charge, low hydrophobicity, and high colloidal stability at physiological conditions. Thus, they should be coated in such a manner so as to minimize any nonspecific binding to the cell surface. PEGylation of nanoparticles has been the most powerful and widely used approach for such a purpose.[48] This study demonstrated that PEGylation reduced the nonspecific interaction of cationic QDs. However, our functionalization scheme would need to be further modified to obtain PEGylated QDs with an even lower surface charge.

Conclusions

We have synthesized various chemically functionalized 20−35 nm QDs, whereby the surface charge and hydrophobicity have been tuned by introducing amine, carboxylate, oleyl, and PEG groups on the QD surface. These surface functional groups significantly influenced the QDs' interaction with the cells. The cationic and hydrophobic QDs have stronger interactions with cells than the anionic QDs. The cationic QDs were the most toxic, but their toxicity could be reduced by introducing PEG on the QD surface. Subcellular localization was also dictated by the functional groups on the QD surface. Hydrophobic QDs labeled the cell membrane and did not enter the cells, but PEGylated cationic QDs entered the cells effectively. QDs have been successfully derived with a balanced hydrophobicity and surface charge to provide for high cellular uptake and low cytotoxicity.

Acknowledgment. The authors thank Dr. Yuangang Zheng for confocal microscopy studies. This work was supported by the Institute of Bioengineering and Nanotechnology (Biomedical Research Council, Agency for Science, Technology and Research, Singapore).

Supporting Information Available: FTIR peaks and assignments of functionalized QDs, raw FACS data of control and functionalized QDs, NMR spectra of functionalized QDs, cytotoxicity of functionalized iron oxide nanoparticles, colocalization study of VI and lysotracker red in HepG2, and cellular interaction of I and oleylamine. This material is available free of charge via the Internet at http://pubs.acs.org.